



# Bioactive Nano-Hydroxyapatite Doped Electrospun PVA-Chitosan Composite Nanofibers for Bone Tissue Engineering Applications

Aishwarya Satpathy<sup>1,2†</sup>, Aniruddha Pal<sup>1†</sup>, Somoshree Sengupta<sup>1</sup>, Ankita Das<sup>2</sup>, Md. Mahfujul Hasan<sup>3</sup>, Itishree Ratha<sup>1</sup>, Ananya Barui<sup>2\*</sup> and Subhadip Bodhak<sup>1\*</sup>

**Abstract** | Combination of bioceramics with polymers to fabricate nanofibrous scaffolds holds enormous potential for bone tissue regeneration. In this study, we aim to incorporate HAp nanoparticles in trace doping amount in PVA-chitosan nanofiber matrix to fabricate PVA-chitosan composite nanofibers with improved performance for application as a bone tissue regeneration material. The diameter of the fabricated composite nanofibrous mat is estimated as  $300 \pm 121$  nm. Beads free nanofibers mat with uniform morphology was ascertained for all sample groups by scanning electron microscopy (SEM) and the overall composition was assessed using Fourier transform infrared spectroscopy (FTIR) and energy dispersive X-ray spectroscopy (EDX). SEM images showed a homogeneous distribution of HAp nanoparticles in the composite nanofibers matrix. Further, X-ray diffraction (XRD) was performed to determine the crystallinity of the fabricated scaffolds. Swelling behavior and hydrolytic degradation of nanofibrous mats were subsequently evaluated by immersing in PBS buffer at pH 7.4 at physiological temperature (37 °C). The biocompatibility study of nanofiber scaffolds was performed with MC3T3 cells. Significantly higher cellular viability was observed on HAp nanoparticles incorporated composite nanofibrous scaffold surface after 7 days of culture in comparison to scaffolds without HAp.

**Keywords:** Bone tissue engineering, Nanohydroxyapatite, Poly(vinyl alcohol), Chitosan, Composite nanofibers, Electrospinning, In vitro cytotoxicity

## 1 Introduction

Bone defects and diseases have increased exponentially in the recent years making them one of the most expansive research areas in the tissue engineering. Available bone substitutes are not sufficiently adequate to meet clinical needs in terms of their functionality, degradation behavior, mechanical strength, and availability or cost while limitations of autologous or heterologous grafts persist<sup>1-3</sup>. Hence, new avenues of tissue engineering are explored with enthusiasm. Specifically, tissue engineered bone constructs have been posed to be advantageous due to their availability, biomimicry, low immunogenicity and

limited secondary trauma in contrast to the clinical grafting process<sup>4-6</sup>. However, the complex, heterogeneous architecture and hierarchy of bone tissue makes fabrication of tissue-mimetic scaffolds challenging<sup>7,8</sup>.

Several fabrication techniques such as freeze drying, phase separation, self assembly and electrospinning have been used for constructing three dimensional biomimetic scaffolds in which the cells are seeded and allowed to populate with secretion of their own extracellular matrix (ECM)<sup>9</sup>. They provide the initial template for regeneration of tissue and help in mimicking the original architecture of ECM<sup>10</sup>. Amongst several

<sup>1</sup> Bioceramics and Coating Division, CSIR-Central Glass and Ceramic Research Institute, 196, Raja S. C. Mullick Road, Kolkata 700032, India.

<sup>2</sup> Centre for Healthcare Science and Technology, Indian Institute of Engineering Science and Technology, Shibpur, Howrah 711103, India.

<sup>3</sup> Institute of Glass & Ceramic Research and Testing (IGCRT), BCSIR, Dhaka 1205, Bangladesh.

\*ananya.pariksha@gmail.com sbodhak@cgcri.res.in

<sup>†</sup>Aishwarya Satpathy and Aniruddha Pal contributed equally to this manuscript.

scaffold types, fibrillar nanostructures resemble natural ECM and provide favorable cell-material interaction. In this regard, electrospinning is one of the widely established fabrication strategies for development of ECM-mimicking nanofibrillar scaffolds<sup>11</sup>. Moreover, the technical simplicity and low tooling costs enhance the acceptability of this method. However, despite several functional advantages inadequate mechanical strength of polymeric nanofibrous scaffolds is still persisted as a key challenge for its widespread applications in load bearing tissue engineered implant applications<sup>12</sup>. Thus, several biological and structural requirements should be taken into consideration while selecting suitable biomaterial for fabrication of scaffolds for tissue engineering. Chitosan, a natural poly- $\beta$ -(1-4)-D-glucosamine in a cationic form that is obtained by partial deacetylation of chitin, attracts a lot of attention due to its biocompatibility, biodegradability, antibacterial and antifungal properties<sup>13</sup>. Several attempts have been made conjugating chitosan with a variety of different biomaterials including calcium phosphate, hyaluronic acid, alginate or other therapeutic cytokines and biomolecules for potential applications in bone tissue engineering<sup>14-18</sup>. Despite such advantages, polycationic nature of chitosan makes it unsuitable for electrospinning. The main problem arises due to the repulsive forces between the polycations, preventing sufficient chain entanglement for forming nanofibers<sup>13</sup>. To overcome this problem, chitosan has been blended with poly (vinyl alcohol) (PVA) which is biodegradable, water soluble and has better nanofiber forming capability<sup>19</sup>. Further, it was suggested that blending with PVA can enhance the thermal stability and mechanical property of electrospun fiber membrane<sup>20</sup>. Several earlier reports have shown synthesis of PVA-chitosan electrospun nanofibers but the right proportion of PVA and chitosan is critical to obtain beadless and uniform fibers morphology<sup>21-23</sup>. It has been shown that with increasing PVA concentration from 10 to 90% in chitosan solution bead formation were reduced and fibers became thicker and more stable.

Here, it can be recalled that natural bone is formed by an “organic matrix-mediated” mineralization process in which collagen fibrils are self-assembled with highly ordered nanosize blade-like hydroxyapatite (HAp) crystal in 50/50 (v/v) or 80/20 (w/w) ratio<sup>24</sup>. Hence, tissue engineered scaffolds or bonegrafts fabricated with only polymer have inherent poor bioactivity and inferior osteoconduction. To address this limitation, several researchers have attempted to make

three-dimensional (3D) nanocomposite scaffolds for bone tissue regeneration by reinforcing higher concentration of nano HAp particles into polymer matrix such as chitosan via porogen leaching method and lyophilization techniques<sup>25-28</sup>. For example, Kashiwazaki et al. fabricated HAp-chitosan porous nanocomposite scaffolds with 80/20 (w/w) blending ratio by porogen leaching method which exhibited good vascularity and bone regeneration capability in small animal model (rat)<sup>25</sup>. Kong et al. has showed that incorporation of nano HAp particles at a much lower concentration (12 wt%) to chitosan scaffold improved proliferation and alkaline phosphatase (ALP) protein expression of mouse osteoblast precursor cells (MC3T3-E1) suggesting potential use of nano-HAp/chitosan composite 3D scaffolds in bone tissue engineering<sup>26</sup>. However, those synthetic bone grafts with higher ceramic contents fail to achieve that structural organization of natural bone tissue and possess poor ductility due to absence of bone-like self-organizing interaction between the HAp and the extra cellular matrix components of the natural bone tissue<sup>24</sup>. Thus, the concentration of HAp phase in the composites have attracted diverse interests, with some studies laying emphasis on use of trace doping amounts of HAp that would facilitate desirable biodegradability and ductility to be better matched with those of natural bone. Consequently, Thein-Han et al. developed bone-like organic-inorganic biomimetic 3D nanocomposite scaffolds consisting of chitosan and varying trace amount of nano HAp particles (0.5, 1, and 2 wt%) for potential use as a bone tissue engineering material. Interestingly, significant increase in compression modulus as well as 1.5 times higher bone cell proliferation can be achieved with incorporation of only 1 wt% HAp nanoparticles into chitosan matrix in comparison to pure chitosan scaffold<sup>27, 28</sup>. However, most of these studies have been performed with freeze dried scaffolds, which do not mimic the nanofibrillar architecture of bone matrix.

In this study, we attempt to incorporate HAp nanoparticles in trace doping levels in PVA-chitosan nanofiber matrix to fabricate PVA-chitosan composite nanofibers with improved performance for application as a bone tissue regeneration material. Such polymer-ceramic composite scaffolds are expected to mimic the structure of natural bones by containing nano-sized HAp particles (at trace concentrations) along with organic nanofiber layers, which provides the site for osteoconduction and the polymeric matrix would facilitate desirable biodegradability and ductility to be better matched with those of natural bone.

To best of our knowledge only a few attempts have been made to incorporate nano HAp particles in trace doping amount in PVA-chitosan electrospun composite nanofibers mat<sup>29, 30</sup>. Amongst them, Celebi et al. reported fabrication of PVA-chitosan electrospun nanofibers consisting of Ag<sup>+</sup>-incorporated HAp nanoparticles (0.1, 0.3, 0.5, and 1.0 wt% of nano HAp reinforcement) which exhibited antibacterial efficiency against *Escherichia coli*<sup>30</sup>. However, beaded fibers morphology and absence of any in vitro bone cell-scaffolds interaction study warrants further process optimization studies to obtain homogeneous and beads free fibrous mat. Thus, much effort has been invested in this work to optimize the blending concentration of polymers (i.e., PVA and chitosan) and ceramic (HAp) phases to produce homogeneous and beads free nanofibrous mat. For this purpose nano HAp was first ultrasonically suspended in aqueous solution and then mixed with the optimized blending ratios of PVA/chitosan spinning solution to fabricate beadless composite nanofibrous mat by conventional electrospinning technique. Physicochemical and structural characterization of the developed nanofibrous mats were further evaluated by XRD, FTIR, SEM, EDX and contact angle measurements. In vitro biocompatibility of composite nanofibrous mat was evaluated by culturing with mouse osteoblast cell line for up to 7 days culture period and compared with virgin PVA and PVA-chitosan electrospun nanofiber scaffolds.

## 2 Materials and Methods

### 2.1 Chemicals

Polyvinyl alcohol (PVA; 60–125 kDa), chitosan (3.8–20 kDa), poly (acrylic acid sodium salt) were procured from Himedia Laboratories Pvt. Ltd., India. Acetic acid glacial (CH<sub>3</sub>COOH) was obtained from Fisher Scientific, USA. Diammonium hydrogen phosphate [(NH<sub>4</sub>)<sub>2</sub>HPO<sub>4</sub>] was bought from Merck, USA. Calcium nitrate tetra-hydrate [Ca(NO<sub>3</sub>)<sub>2</sub>·4H<sub>2</sub>O], di-ammonium hydrogen ortho- phosphate [(NH<sub>4</sub>)<sub>2</sub>HPO<sub>4</sub>], triethanolamine (TEA) and ammonium hydroxide (NH<sub>4</sub>OH) were procured from SD Fine-Chem, India. Ultra pure water (UPW) was used throughout all the processes and obtained using a Milli Q-System (Milli Q Academic Century, ZMQS50001, USA).

### 2.2 Preparation of Nano-Hydroxyapatite (nHAp) Powder

The nano HAp powder was prepared in house by following a wet chemical method using

analytical reagent grade Ca(NO<sub>3</sub>)<sub>2</sub>·4H<sub>2</sub>O and (NH<sub>4</sub>)<sub>2</sub>HPO<sub>4</sub> as precursors of calcium and phosphate ions, respectively as described in our earlier work<sup>31</sup>. Briefly, 100 mL of 1(M) solutions of Ca(NO<sub>3</sub>)<sub>2</sub>·4H<sub>2</sub>O was taken into a 1 l beaker and stirred vigorously using a magnetic stirrer at 750 rpm in room temperature. Then, 100 mL of 0.6 (M) of TEA (capping agent) was added dropwise to the Ca(NO<sub>3</sub>)<sub>2</sub>·4H<sub>2</sub>O solution at a rate of 3–5 mL/min under vigorous stirring condition. Following, 0.6 (M) of (NH<sub>4</sub>)<sub>2</sub>HPO<sub>4</sub> solution was added dropwise into the beaker. The pH of the solution was always maintained at 10–12 by dropwise addition of ammonium hydroxide (NH<sub>4</sub>OH) solution during mixing of TEA and (NH<sub>4</sub>)<sub>2</sub>HPO<sub>4</sub> into Ca(NO<sub>3</sub>)<sub>2</sub>·4H<sub>2</sub>O solution. The Ca:P molar ratio of Ca(NO<sub>3</sub>)<sub>2</sub>·4H<sub>2</sub>O and (NH<sub>4</sub>)<sub>2</sub>HPO<sub>4</sub> solution was kept as 1.67 in order to obtain stoichiometric nano HAp powder. Following this, the mixture was stirred for another 30 min at room temperature and then allowed to precipitate for 48 h. Finally, the gelatinous precipitate was collected and washed thoroughly by using UPW in a centrifuge (Heal Force Neofuge 18R, Shanghai Lishen Scientific Equipment Co. Ltd., China) at 5000 rpm with 5 min interval until the ammonia smell is completely removed. Afterwards, the white HAp precipitate was dried in the oven at 70 °C overnight, and subsequently ball milled (Retsch GmbH, Germany) for 24 h in UPW medium in which certain amount of poly (acrylic acid sodium salt) was added as deflocculating agent. After ball milling, HAp powder was dried in the oven at 70 °C overnight to obtain nanosized HAp powder. Finally, the dried nano HAp powder was ground in an agate mortar pestle to break any agglomeration and subsequently used in physicochemical characterizations and fabrication of HAp incorporated PVA-chitosan nanofibers by electrospinning technique.

### 2.3 Fabrication of PVA, PVA-CHT and HAp Incorporated PVA-CHT Composite Nanofibers Mat

Pre-blending concentration of PVA solution (i.e., 15% (w/v) PVA solution in ultra-pure water) and chitosan solution (i.e., 1% (w/v) chitosan solution in 1% (v/v) acetic acid) is being selected based on previous studies and process optimizations in order to produce homogeneous and beads free nanofibrous mat<sup>22, 23</sup>. At first, 15% (w/v) PVA solution was prepared by mixing PVA in UPW at 70 °C for 6 h using a magnetic stirrer at 600 rpm. Then, 1% (w/v) chitosan solution was made in 1% (v/v) acetic acid in UPW and

kept under constant stirring at 600 rpm for 24 h to obtain a clear solution. In our preliminary studies, two different PVA/chitosan blend ratio i.e., 80:20 and 90:10 (v/v) have been explored, and fibrous mat quality was found superior at PVA-chitosan blending ratio 90:10 (v/v) under optimized spinning conditions. Consequently, we have selected PVA/chitosan (PVA-CHT) blending ratio 90:10 (v/v) as the final blend in this study and PVA-CHT solution was prepared by mixing the appropriate volume of stock 15% (w/v) PVA solution and 1% (w/v) chitosan solution and stirred for 30 min at 600 rpm in room temperature to achieve homogenous mixture.

In this study, we aimed at fabrication of composite electrospun nanofibrous mat by incorporating bioactive HAp nanoparticles in a trace doping amount into PVA-chitosan matrix and compared its microstructural, physicochemical as well as in vitro bone cell-materials interactions with PVA and PVA-chitosan nanofibers pertinent to bone tissue engineering applications. Thus in our preliminary studies, two different concentration of nano HAp (0.5 and 1.0 wt%) were investigated for incorporation into PVA/Chitosan (90:10 v/v) nanofibrous mat based on previous studies and found 0.5 wt% HAp reinforcement as optimal composition in view of beadless fibers morphology and bone cell proliferation<sup>29, 30</sup>. Consequently, a fixed concentration (i.e., 0.5 wt%) of nano HAp powder was selected to incorporate into the PVA-CHT polymer matrix for fabrication of HAp/PVA-CHT composite fibers and subsequent physicochemical and in vitro biological characterizations. For that purpose, nano HAp powder (nHAp) was first suspended in aqueous solution (UPW) supplemented with minute quantity of deflocculating agent ((acrylic acid sodium salt) and thoroughly mixed at 300 rpm for 1 h followed by the ultrasonication for 10 min. Then, desired volume of ultrasonicated HAp stock solution was mixed with blended polymer solution (PVA-CHT) to prepare nano HAp/PVA-CHT spinning solution (0.5 wt% HAp, w/v) and vigorously stirred for 2 h to achieve homogeneous distribution of nano HAp powder in polymer blend solution.

The PVA, PVA-CHT and 0.5 wt% nano HAp incorporated PVA-CHT (0.5. HAp/PVA-CHT) composite nanofibers were fabricated by electrospinning technique (E-SPIN Nanotech Pvt. Ltd., IIT Kanpur, India). 10 mL each group of solution was filled into a 5 mL syringe with a stainless steel needle for electrospinning. Then, the electrospinning process was carried out at room temperature with a constant feeding rate of 1 mL/h and

the distance between the needle tip and collector was kept at 14 cm. The aluminum foil was used as the collector for the nanofibers. The applied voltage was varied between 20 and 25 kV to obtain beadless and uniform nanofibers mat. Extensive preliminary studies were carried out to optimize the electrospinning parameters in order to obtain reproducible, uniform and beadless nanofibers. At the end of spinning process, each group of the fibrous mat was collected from the aluminium foil, dried and stored in a vacuum dessicator for further characterizations.

## 2.4 Characterization of the Samples

X-ray diffraction (XRD) pattern of as prepared nano HAp powder and electrospun nanofiber mats was determined by a X-ray Diffractometer (X'Pert Pro MPD Diffractometer, Panalytical, Alnelo, Netherlands) with scanning range 0°–60° to assess different crystalline phases and structures. Fourier Transform Infrared (FTIR) spectroscopy (IRAffinity-1S, IRAffinity-1, MIRacle 10, SHIMADZU, Japan) was carried out for analyzing the molecular fingerprints of different test samples. The surface morphologies and elemental composition analysis of nano HAp powder and electrospun fibrous mats were studied by Scanning electron microscopy (SEM) and Energy dispersive X-ray (EDX) analyses (Phenom ProX, Phenom World B.V., Netherlands). Surface properties for different sample groups was assessed by measuring the static contact angles of sessile drops of DI water using a face contact angle setup equipped with a camera (Surface tensiometer surfactens 4.5, OEG GmbH, Germany). For this purpose, 2 mL polymer blend solution from each of sample group (PVA, PVA-CHT, and 0.5HAp/PVA-CHT) was taken in a 5 mL syringe and drop casted into film on a glass slide and subsequently air dried prior contact angle measurement. Minimum three measurement was carried out on triplicate samples for each group and the average contact angle values were calculated.

## 2.5 Swelling Behavior of PVA, PVA-CHT and 0.5HAp/PVA-CHT Nanofibrous Mat

Swelling behavior of PVA, PVA-CHT, and 0.5HAp/PVA-CHT nanofibrous mats was assessed by immersing in PBS buffer at pH 7.4 at physiological temperature (37 °C). Briefly, nanofibrous mats were cut into 20 × 20 mm<sup>2</sup> test specimen and each sample was immersed into 50 mL phosphate buffer solution (pH 7.4) at 37 °C in an incubator up to 16 h (960 min). Prior immersion,

initial dry weight ( $W_d$ ) of each test specimen was measured. After specific time intervals, nanofibrous mats were taken out of PBS buffer and carefully removed the surface water by holding over tissue paper for a few seconds. Subsequently, the swell weight ( $W_s$ ) of each test specimen was measured. The experiment was done in triplicates for each scaffold. The swelling ratio (%) was calculated using Eq. 1 by gravimetric method<sup>32</sup>.

$$\text{Swelling ratio (\%)} = \frac{W_s - W_d}{W_d} \times 100 \quad (1)$$

where,  $W_d$  stands for initial dry weight and  $W_s$  refers to swell weight of the nanofibrous mat at respective time point.

## 2.6 Hydrolytic Degradation of PVA, PVA-CHT and 0.5HAp/PVA-CHT Nanofibrous Mat

Hydrolytic degradation of PVA, PVA-CHT, and 0.5HAp/PVA-CHT nanofibrous mats was evaluated by immersing in PBS buffer at pH 7.4 at physiological temperature (37 °C) for 1, 4 and 7 days time point. Briefly, nanofibrous mats were cut into 20 × 20 mm<sup>2</sup> pieces for each sample group and dry weight of each test specimen was measured ( $W_o$ ). Following this, each sample was immersed in 50 mL phosphate buffer solution (pH 7.4) and kept in an incubator at 37 °C. After specific time intervals, samples were taken out of PBS buffer and dried in an oven at 55 °C. Subsequently, dried weight ( $W_t$ ) of each test sample was measured and the weight loss (%) was calculated using Eq. 2 by gravimetric method<sup>33</sup>. The experiment was done in triplicates for each scaffold.

$$\text{Weight loss (\%)} = \frac{W_o - W_t}{W_o} \times 100 \quad (2)$$

where,  $W_o$  stands for initial weight and  $W_t$  refers to dry weight of the nanofibrous mat at respective time point.

## 2.7 In vitro Bone Cell–Material Interactions

In vitro biocompatibility of different electrospun nanofiber mats (PVA, PVA-CHT and 0.5HAp/PVA-CHT) was evaluated using mouse osteoblast cell line (MC3T3-E1, ATCC, USA). All three groups of nanofibrous mats were cut into small test specimen (10 mm × 10 mm) and sterilized by immersing in 70% EtOH for 30 min, followed by rinsing with sterile UPW for 15 min and ultraviolet (UV) exposure for 1 h in aseptic condition. The MC3T3 cells as used in the study

were prepared by culturing in  $\alpha$ -MEM growth medium (Gibco, USA) supplemented with 10% fetal bovine serum (FBS) and 1% antibiotic–antimycotic solution in a T75 tissue culture flask (Himedia Laboratories Pvt. Ltd., India). The cultured cells were kept in the incubator (Cell-Culture, ESCO) at 37 °C with 5% CO<sub>2</sub> and 95% humidity and the culture medium was replaced with fresh medium at every 2–3 days. Following this, the confluent cells were trypsinized (trypsin/EDTA; Invitrogen Corporation, USA), and cell suspensions were prepared. Finally, cells were seeded on the surface of nanofiber mats at a density of 10,000 cells/sample placed in a 24-well cell culture plate by adding 100  $\mu$ L of cell suspension to each sample and incubated for 4 h in the incubator at 37 °C for cell adherence. After that, 1 mL  $\alpha$ -MEM growth medium supplemented with 10% FBS and 1% antibiotic–antimycotic was added to each well. Cultures were maintained up to 7 days in the incubator at 37 °C under an atmosphere of 5% CO<sub>2</sub> and 95% humidity and culture media were changed every 2 days. Samples were then collected after specific time interval to study the cell proliferations and morphology.

### 2.7.1 Cell Proliferation Using the MTT Assay

In vitro cytotoxicity of different nanofibrous mats was quantitatively assessed and compared by measuring the viable cell proliferation on different sample surfaces after 1, 3 and 7 days culture timepoint using the MTT assay kit (Sigma Aldrich, USA). Briefly, the MTT reagent [3-(4,5-dimethylthiazol-2-yl)-2,5-diphenyl tetrazolium bromide] was dissolved in phosphate buffer solution (PBS, Gibco) at a concentration of 5 mg/mL. After the specified incubation timepoint, freshly prepared MTT solution was mixed with culture media in a volume ratio of 1:9. After mixing, 1 mL of solution was added to each sample. The mitochondrial succinate dehydrogenase reduced MTT to a dark purple formazan product. After 3 h incubation, the formazan crystals was saturated in 500  $\mu$ L of DMSO (Dimethyl sulfoxide, Sigma) solution. An aliquot of 100  $\mu$ L was transferred into a 96-well plate and optical density was measured using a plate reader (iMark, Bio-Rad) at 595 nm. Triplicate samples ( $n=3$ ) were used in MTT assay to ensure reproducibility. Cell proliferation (%) was calculated by normalizing the measured optical density of each sample group to measured optical density of PVA for that particular culture time point (data not shown).

### 2.7.2 Cell Morphology by Fluorescence Imaging

Cell morphology was qualitatively analyzed after 7 days culture period by staining the cell nuclei with a fluorescent dye DAPI (4',6-diamidino-2-phenylindole Catalogue No: D1306, Thermo Fisher) and counterstaining the cell membrane and cytoplasmic proteins with another fluorescent dye FITC (Fluorescein isothiocyanate isomer I, Thermo Fisher) followed by fluorescence imaging. Briefly, after 7 days incubation period the samples ( $n=2$ , duplicate condition) cultured with MC3T3-E1 cells were rinsed with 1X PBS for 3 times/5 min each, fixed in 3.7% formaldehyde for 10 min. This was followed by 3 times wash in PBS. Later the cells were permeabilized by immersion in 0.2% Triton X-100 for 5 min. Triton X was aspirated followed by washing with PBS. Then FITC staining solution (2.5  $\mu\text{g}/\text{mL}$ ) was added to each sample well and kept for 5 min and then washed with PBS. Lastly, the cells were imaged ( $\lambda_{\text{ex}} \sim 359 \text{ nm}$ ,  $\lambda_{\text{em}} \sim 461 \text{ nm}$  when FITC is bound to cytoplasm) under reflected light fluorescence microscope (OlympUSBX51TRF, Tokyo, Japan).

### 2.8 Statistical Analysis

Data for contact angle and MTT assay are presented as mean  $\pm$  standard deviation. Statistical analysis was performed on MTT assay results using student's  $t$  test and  $P$  value  $< 0.05$  was considered significant.

## 3 Results and Discussion

### 3.1 SEM Morphology and EDX Elemental Analyses

SEM morphology of as synthesized nano HAp powders (nHAP) and representative elemental analysis (EDX analysis) results are presented in Fig. 1a, b, respectively. Evidently, granular HAp nanoparticles with an average particle size below 100 nm was obtained by wet chemical precipitation method (Fig. 1a). Presence of some agglomerates can also be seen due to high surface energy of the nano-sized HAp particles. EDX spectrum results acquired from the HAp particles further confirmed the presence of Ca, P and O elements indicating the HAp chemical composition (as shown in Fig. 1b). Morphologies of electrospun virgin PVA, PVA-CHT blend and 0.5HAp/PVA-CHT composite nanofibrous mats are presented in Fig. 1c–e, respectively. A beads-free continuous and nonwoven structure with interconnected porous morphology can be seen for all the electrospun nanofibrous mats irrespective of their composition. Pure or virgin PVA nanofibers

were smooth and homogeneous but bimodal in nature with an average diameter of  $440 \pm 196 \text{ nm}$  (Fig. 1c). In case of PVA-chitosan blend (PVA-CHT) nanofibers were more uniform with an average diameter of  $395 \pm 162 \text{ nm}$  as it is believed that the functional groups of chitosan formed hydrogen bonds with PVA to give more stability and defect-free nanofibers morphology (Fig. 1d). In case of composite nanofibers (0.5HAp/PVA-CHT) successful incorporation of HAp nanoparticles was seen in the form of aggregated mass inside the PVA-CHT blend polymer nanofibers matrix. Average nanofibers diameter was reduced to  $300 \pm 121 \text{ nm}$  for composite nanofibers (0.5HAp/PVA-CHT) with the incorporation of HAp nanoparticles (Fig. 1e) and the surface of fibers was rougher than that of pure polymer fibers due to the inclusion of HAp nanoparticles. It can be recalled that a rough nanofiber surface produced by the embedded HAp nanoparticles is expected to increase surface wettability and promote bone cell attachment and osteogenic differentiation<sup>34</sup>. Incorporation of the HAp nanoparticles can be confirmed from the associated elemental analysis results (EDX) acquired from the embedded particles into the polymer nanofibers matrix (as shown in Fig. 1f).

### 3.2 FTIR Analysis

The FTIR spectra of nano HAp powder and electrospun PVA, PVA-CHT and 0.5HAp/PVA-CHT nanofibers are presented in Fig. 2a. In case of nano HAp powder, broad peaks at  $3450 \text{ cm}^{-1}$  and  $1644 \text{ cm}^{-1}$  are mainly due to adsorbed water<sup>35</sup>. Further, phosphate stretching mode, phosphate bending mode were seen at  $1034 \text{ cm}^{-1}$  and  $605 \text{ cm}^{-1}$  respectively<sup>36,37</sup>. Besides, C–O stretching vibration of  $\text{CO}_3^{2-}$  were found at  $1454 \text{ cm}^{-1}$  and  $1414 \text{ cm}^{-1}$ , respectively. These characteristic peaks suggested successful synthesis of HAp. In pure PVA nanofibers FTIR spectra, two peaks were obtained at  $3300 \text{ cm}^{-1}$  and  $1640 \text{ cm}^{-1}$  for O–H stretching vibration and bending vibration, respectively. The FTIR spectra of PVA-CHT nanofibers revealed the band at  $1430 \text{ cm}^{-1}$  due to amide bond (amide-II) of chitosan that did not appear in the pure PVA spectra<sup>38</sup>. In 0.5HAp/PVA-CHT composite nanofibers, besides the PVA-CHT characteristics peaks at  $3300 \text{ cm}^{-1}$  is due to –OH stretching vibration. Besides, the amide bond (amide-II) of CHT and C–O stretching vibration peak of  $\text{CO}_3^{2-}$  of nHAP were merged and was found at  $1423 \text{ cm}^{-1}$  with high intensity. Additional peaks were observed at  $1096 \text{ cm}^{-1}$  and  $615 \text{ cm}^{-1}$ . These additional bands

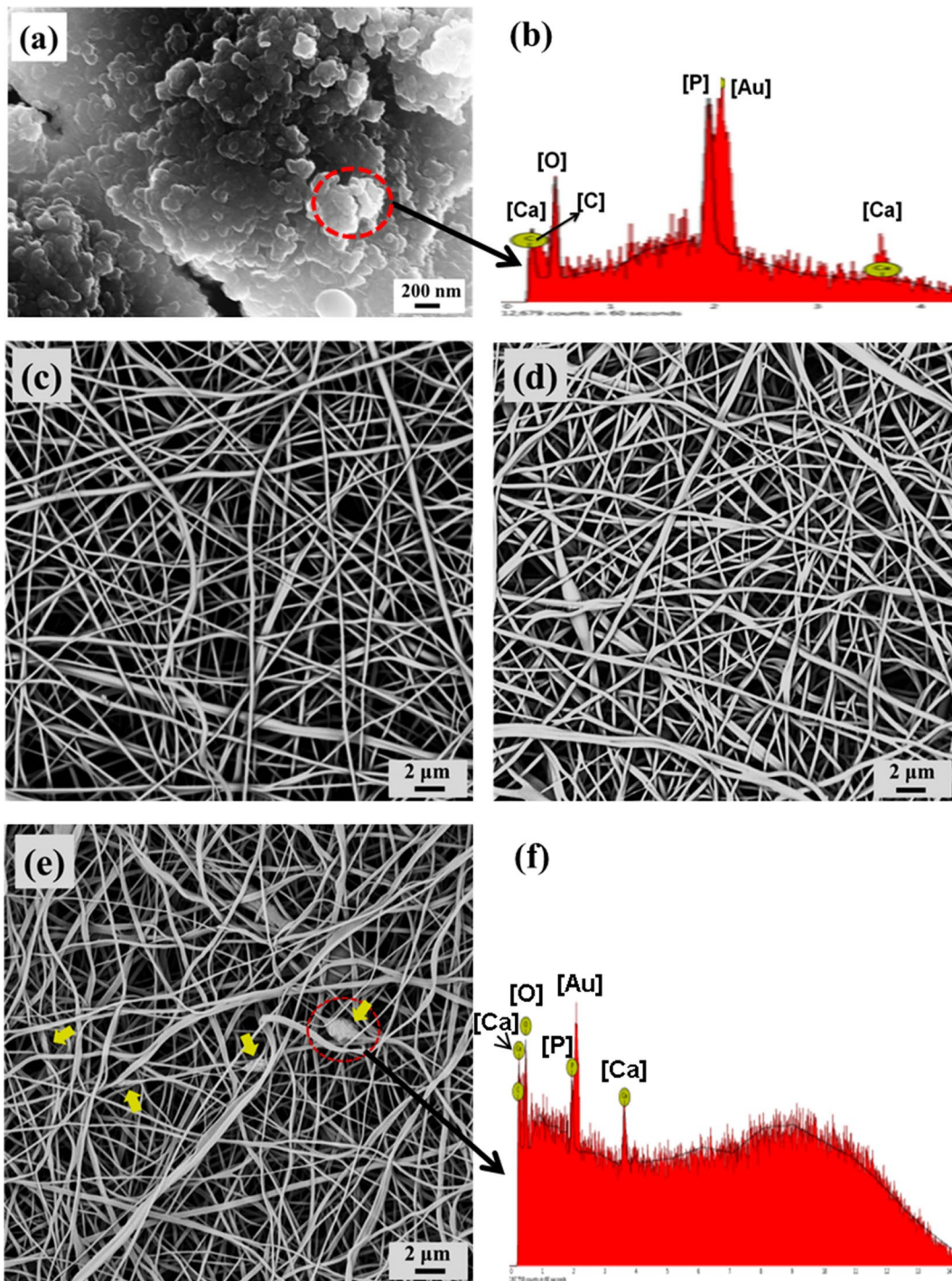


**Figure 1:** SEM micrographs illustrating the powder morphology of **a** as synthesized nano HAp (nHAP) dried at 70 °C for overnight, and surface morphology of electrospun **c** PVA, **d** PVA-CHT and **e** 0.5HAp/PVA-CHT nanofibers. EDX elemental analysis results showing chemical composition of **b** nano HAp powder (nHAP) and **f** 0.5HAp/PVA-CHT composite nanofibers. (small arrows are indicating the incorporated HAp nanoparticles into nanofibers matrix).

are assigned to the characteristic peaks of HAp confirming the presence of HAp nanoparticles into composite nanofibers. Overall, FTIR analyses results suggest the plausible incorporation of

HAp nanoparticles into the polymer matrix for successful fabrication of 0.5HAp/PVA-CHT composite nanofibers.

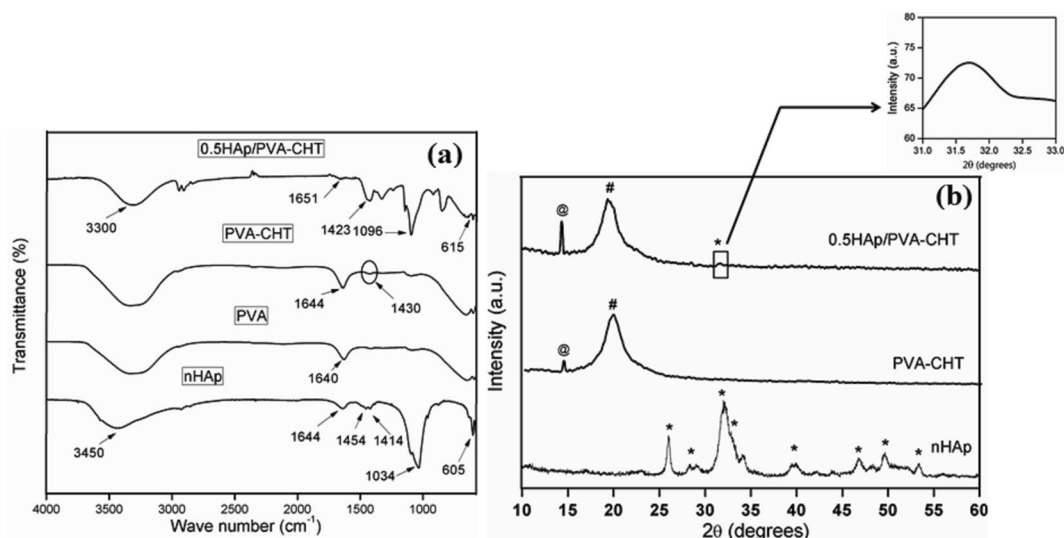


**Figure 2:** **a** FTIR spectra of nano HAp powder (nHAP) and electrospun PVA, PVA-CHT, 0.5HAp/PVA-CHT nanofibers, **b** XRD patterns of nano HAp powder (nHAP) and electrospun PVA, PVA-CHT, 0.5HAp/PVA-CHT nanofibers. The inset shows the XRD peak corresponding to the HAp phase for 0.5HAp/PVA-CHT composite nanofibers (\*Peak corresponding to HAp phase, #Overlapping peaks corresponding to both PVA and chitosan, @Artifact from sellotape that was used for fixing the nanofiber mat in sample holder during XRD analysis).

### 3.3 XRD Analysis

The phase of the HAp powders and fabricated electrospun nanofibrous mats was confirmed by X-ray diffraction analysis. Figure 2b shows the XRD patterns for as synthesized nano HAp powder dried at 70 °C along with PVA-chitosan and HAp incorporated PVA-chitosan composite nanofibers. Evidently, the four major peaks in as-synthesized HAp powder XRD pattern at 31.8°, 32.54°, 26.12° and 34.23° are the diffraction peaks from (211), (112), (002) and (202) planes and matching well with the JCPDD PDF No. 9-432<sup>39</sup>. From this observation it can be inferred that phase pure HAp powder was prepared under the present experimental conditions. In addition, extensive peak broadening and overlapping of the diffraction reflections, as in the case of natural bone, suggesting nano sized and low crystallinity of the HAp particles<sup>40</sup>. In case of PVA-chitosan nanofibers, (PVA-CHT) the broad peak at about 20° is assigned to the overlapping peaks of both PVA and chitosan and was indicative of successful blending of PVA onto the backbone of chitosan moiety<sup>41</sup>. The XRD pattern of HAp incorporated PVA-CHT composite nanofibers shows the presence of broad (211) diffraction peak of between 31° and 32° confirming the presence of HAp phase along with characteristic peak of PVA-chitosan blend at 20°. This decrease in HAp crystallinity as evident from broader HAp peak may be caused by the presence of the chitosan matrix and

trace amount of HAp content (0.5 wt%, w/v) in the composite nanofibers. A similar observation was also reported by Wang et al.<sup>42</sup>. Overall, XRD analyses results are also in good agreement with SEM, EDX and FTIR observation HAp nanoparticles are being successfully incorporated into the PVA-chitosan nanofiber matrix.

### 3.4 Contact Angle Measurement

Wettability of different samples was assessed by measuring the static contact angles of sessile drops of DI water on PVA, PVA-CHT, 0.5HAp/PVA-CHT drop casted films. The films were prepared from each of spinning solutions and used as specimen instead of nanofibrous mats which were not suitable for accurate measurement due to their inherent porous structure. The comparative plot of water contact angle as measured for PVA, PVA-CHT and 0.5HAp/PVA-CHT samples are presented in Fig. 3a. Overall, all the sample groups are found to be hydrophilic in nature which is beneficial for bone cell attachment and proliferations. The average contact angle of pure PVA was found to be at  $18.9^\circ \pm 0.78^\circ$  whereas PVA-CHT exhibited increased wettability or reduced water contact angle of  $16.63^\circ \pm 0.25^\circ$  due to the availability of -OH group in the saccharides moieties in chitosan<sup>43</sup>. Interestingly, 0.5HAp/PVA-CHT composite exhibited maximum wettability amongst all samples with a



lowest contact angle value of  $12.53^\circ \pm 0.25^\circ$ . It is believed that increased surface roughness due to the exposure of HAp nanoparticles might have helped to increase its hydrophilicity<sup>44</sup>. Digital pictures of water contact angles as measured for different samples are in good agreement clearly showed more spreading of water droplet on HAp incorporated PVA-CHT composite surface in comparison to pure PVA and PVA-CHT samples.

### 3.5 Swelling Behavior of PVA, PVA-CHT and 0.5HAp/PVA-CHT Nanofibrous Mat

The swelling behavior of the nanofibrous mat plays an important role in cellular adhesion and proliferation as it influences the fluid intake capacity of the scaffold. Figure 3b shows the swelling behavior of PVA, PVA-CHT and 0.5HAp/PVA-CHT nanofibrous mat after immersing in PBS buffer up to 960 min (16 h) at pH 7.4 at physiological temperature (37 °C). It can be noted that the increase in weight after immersion in PBS buffer indicates the swelling behavior of the nanofibers and the swelling ratio (%) was calculated by normalizing the increased weight for swelling to initial dry weight of nanofibrous mat. The degree of swelling was evidently increased for PVA-CHT in comparison to PVA, while 0.50HAp/PVA-CHT sample showed maximum swelling amongst all groups. Interestingly, maximum swell ratio (%) of 130.18%, 142.42% and 194.02% could be achieved for PVA, PVA-CHT, and 0.50HAp/PVA-CHT, respectively after 810 min (13.5 h) immersion period. It is believed that incorporation of chitosan leads to increase

in hydrophilicity of PVA-CHT nanofibers due to the presence of functional amino and hydroxyl groups in chitosan<sup>45</sup>. Additionally, the incorporation of nano HAp into composite nanofibers has further increased the hydrophilic nature of the scaffolds due to presence of hydroxyl groups in HAp group that increases the buffer solution intake. This observation is in good agreement with contact angle results which has markedly confirmed that 0.5HAp/PVA-CHT composite possesses maximum wettability amongst all samples (Fig. 3a). However, the swelling ratio (%) was found to be decreased after 810 min (13.5 h) indicating the degradation and leaching of polymers by dissolution that resulted in the decrease in swelling ratio<sup>45</sup>. Similar results were also reported by other researchers when HAp was incorporated into chitosan/PLA blend and BisGMA<sup>46,47</sup>.

### 3.6 Hydrolytic Degradation of PVA, PVA-CHT and 0.5HAp/PVA-CHT Nanofibrous Mat

Hydrolytic degradation is an important useful process that influences scaffolds biodegradability and strength to support cell proliferation and new tissue formation. The hydrolytic degradation behavior of PVA, PVA-CHT and 0.5HAp/PVA-CHT nanofibers after immersing in PBS buffer up to 7 days at pH 7.4 at physiological temperature (37 °C) is shown in Fig. 3c. Decrease in scaffold weight after immersion in PBS buffer specifies the hydrolytic degradation behavior of the nanofibers and weight loss (%) was calculated by gravimetric method. From Fig. 3c it can be observed that after day 1 the % weight loss was 5.9%, 8.30%,

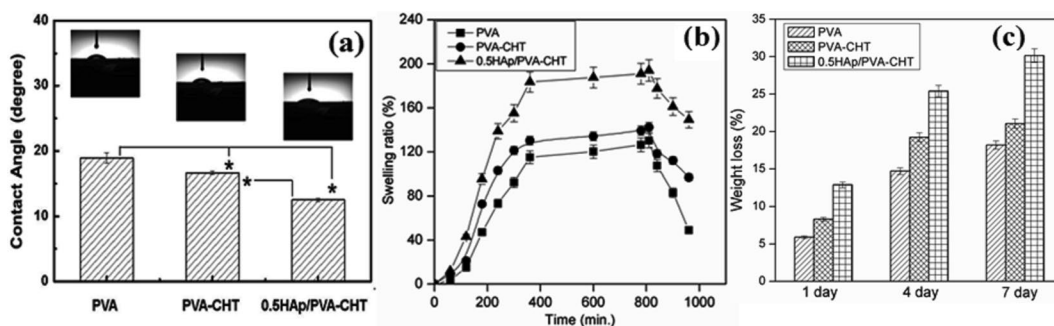


**Figure 3:** **a** Water contact angles as measured on PVA, PVA-CHT, 0.5HAp/PVA-CHT drop casted films. Digital pictures of water contact angles as measured for different samples are presented in the insets. Statistical analysis indicates that the differences in contact angles among various samples are significant ( $*P < 0.05$ ,  $n = 9$ ), **b** swelling ratio of PVA, PVA-CHT and 0.5HAp/PVA-CHT nanofibrous mat after immersing in PBS buffer up to 960 min (16 h) at pH 7.4 at physiological temperature (37 °C), **c** hydrolytic degradation behavior of PVA, PVA-CHT and 0.5HAp/PVA-CHT nanofibers after immersing in PBS buffer up to 7 days at pH 7.4 at physiological temperature (37 °C).

and 12.90% for PVA, PVA-CHT, and 0.5HAp/PVA-CHT scaffolds, respectively. It is believed that the increase in weight loss for HAp incorporated nanofibrous scaffolds over PVA-CHT and PVA is because of higher scaffold hydrophilicity which leads to higher buffer solution uptake that promotes hydrolysis. Similarly, incorporation of chitosan into PVA moiety for PVA-CHT scaffold increases the hydrophilic nature of the nanofibers that promotes degradation. Further, higher buffer solution uptake also accelerates the erosion and diffusion of chitosan. This rapid degradation process during the initial period is matching well with wettability and swelling behavior of different scaffolds as presented in Fig. 3a, c, respectively. From Fig. 3c it can be clearly seen that the rate of degradation is reduced with increasing the immersion time period as the % weight loss was found 14.40% and 18.18% (PVA), 19.23% and 21.05% (PVA-CHT), 25.39% and 30.15% (0.5HAp/PVA-CHT) at day 4 and day 7, respectively. This decrease in degradation rate with increasing immersion period can be attributed to the stabilization in hydrolysis kinetics and lower buffer solution intake mechanism. Overall, the observed hydrolytic degradation behavior of all nanofibrous scaffolds is typical of other biodegradable natural polymers<sup>48, 49</sup> Similar results were also reported for other HAp incorporated polymer nanocomposite scaffolds<sup>50, 51</sup>. The effect of chitosan and HAp nanoparticles in degradation behavior of scaffolds is an important finding and scaffolds degradation rate can be potentially controlled by controlling their compositions for patient specific applications. In addition, scaffolds stability can also be improved by using suitable cross-linkers<sup>52</sup>.

### 3.7 In Vitro Bone Cell–Material Interactions

Cellular viability on different scaffold composition was assessed through the MTT assay (Fig. 4a). Viability of osteoblast cells markedly increased after 3 days of culture in all study groups in comparison to that of 1 day culture. However, no significant difference in cell viability was observed among all three study groups at 3 days culture period. Interestingly, after 7 days of culture the viability and proliferation of osteoblast was significantly increased in 0.5HAp/PVA-CHT nanofibers in comparison to PVA-CHT nanofibers and control pure PVA nanofibers groups. It has been observed that 0.5HAp/PVA-CHT fibers showed a maximum 2.76 fold increase in cell proliferation in comparison

to PVA nanofibers after 7 days of culturing. On the other hand, PVA/CHT nanofibers also showed a moderate 1.40 fold increase in cell proliferation with respect to PVA fibers at the same time point. Most importantly, doping of nano HAp showed a 1.98 fold increase in bone cell proliferation when comparison is made between 0.5HAp/PVA-CHT and PVA-CHT nanofibers after 7 days culture period. Such increasing trend in cellular viability in nHAp composite scaffolds indicate the possibility of release of  $\text{Ca}^{2+}$  and  $\text{PO}_4^{3-}$  ions from the construct could potentially create conducive environment for better bone cell proliferation over other polymeric scaffolds groups. In addition, hydrophilic surfaces of composite nanofibrous scaffolds are expected to favor cell adhesion as well as enhance ionic interactions between cell and fibers leading to accelerated cell proliferation. Further, qualitative FITC fluorescence cell morphology results (as shown in Fig. 4b) indicate maximum cellular adhesion and proliferation in 0.5HAp/PVA-CHT nanofibrous mat surface at 7th day of culture in comparison to other sample groups. Evidently, this observation is in good agreement with quantitative MTT

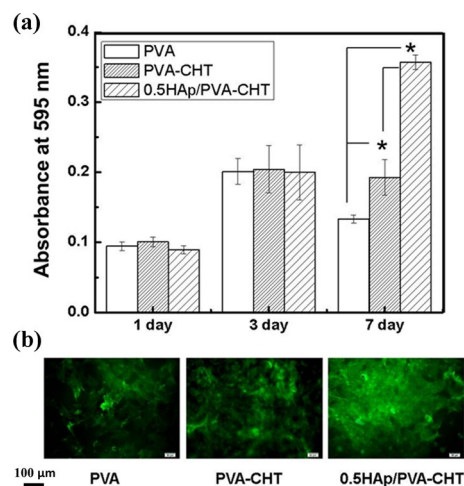


**Figure 4:** **a** Optical density measurement illustrating mouse osteoblast (MC3T3-E1) cell proliferation on different nanofibrous mat surfaces after 1, 3, and 7 days culture period. Statistical analysis indicate that the differences in cell densities among various samples are significant at 7 days timepoint ( $*P < 0.05$ ,  $n = 3$ ), **b** Fluorescence micrographs showing morphology of MC3T3-E1 cells stained with FITC on electrospun PVA, PVA-CHT, 0.5HAp/PVA-CHT nanofibrous mat surfaces after 7 days culture timepoint.

assay results. In support of beneficial effects on the developed composite fibers in bone tissue engineering, researchers have also reported that incorporation of doping concentration (5 wt%) of nano HAP particles in hydrogel matrices result in increased extracellular matrix production by stem cells reflected by increase in both elastic modulus as well as formation of extracellular matrix components<sup>53</sup>.

#### 4 Conclusions

In present study, HAP nanoparticles doped electrospun PVA-chitosan composite nanofibrous mat was successfully fabricated with improved performance for potential application as a bone tissue regeneration material. The SEM and EDX images showed successful encapsulation of HAP nanoparticles into the composite nanofibrous scaffolds. FTIR spectra exhibited the molecular fingerprints of composite scaffolds and further confirmed the successful fabrication of HAP incorporated polymer scaffolds. Besides, incorporation of nano HAP improved the hydrophilicity as well as swelling behavior of composite scaffolds and significantly enhanced the proliferation of osteoblast cells. Further, the rate of in vitro hydrolytic degradation was also found to be decreased for all sample groups with increasing immersion period. Maximum viability and good surface coverage of MC3T3 cells on composite scaffold surfaces have been observed after 7 days of culture. Overall the study suggests the incorporation of HAP nanoparticles improves the biocompatibility as well as bioactivity of PVA-chitosan composite scaffolds for osteoblast and such composite scaffolds may serve as a good template for bone tissue engineering.

#### Publisher's Note

Springer Nature remains neutral with regard to jurisdictional claims in published maps and institutional affiliations.

#### Acknowledgements

The authors would like to acknowledge the Ramalingaswami Re-Entry Fellowship, Department of Biotechnology (DBT), Government of India (BT/RLF/Re-entry/13/2016) and Science and Engineering Research Board (SERB), Department of Science & Technology, Government of India (PDF/2018/000182) for financial support.

Received: 6 June 2019 Accepted: 8 August 2019  
Published online: 20 August 2019

#### References

1. Baroli B (2009) From natural bone grafts to tissue engineering therapeutics: brainstorming on pharmaceutical formulative requirements and challenges. *J Pharm Sci* 98:1317–1375
2. Dimitriou R, Jones E, McGonagle D (2011) Bone regeneration: current concepts and future directions. *BMC Med*. 9:66
3. Soucacos PN, Johnson EO, Babis G (2008) An update on recent advances in bone regeneration. *Injury* 39S2:S1–S4
4. Basu B (2017) *Biomaterials science and tissue engineering, principles and methods*. Cambridge University Press, Cambridge
5. Bodhak S, Kikuchi M, Sogo Y, Tsurushima H, Ito A, Oyane A (2013) Calcium phosphate coating on a bioresorbable hydroxyapatite/collagen nanocomposite for surface functionalization. *Chem Lett* 42:1029–1031
6. Bodhak S, De Castro LF, Kuznetsov SA, Azusa M, Bonfim D, Robey PG Jr, Simon CG (2018) Combinatorial cassettes to systematically evaluate tissue-engineered constructs in recipient mice. *Biomaterials* 186:31–43
7. Guerado E, Caso E (2017) Challenges of bone tissue engineering in orthopaedic patients. *World J Orthop* 8:87–98
8. Turnbull G, Clarke J, Picard F, Riches P, Jia L, Han F, Li B, Shu W (2018) 3D bioactive composite scaffolds for bone tissue engineering. *Bioact Mater* 3:278–314
9. Ghassemi T, Shahroodi A, Ebrahimzadeh MH, Mousavian A, Movaffagh J, Moradi A (2018) Current concepts in scaffolding for bone tissue engineering. *Arch Bone Jt Surg* 6:90–99
10. Chen D, Sarkar S, Candia J, Florczyk SJ, Bodhak S, Driscoll MK Jr, Simon CG, Dunkers JP, Losert W (2016) Machine learning based methodology to identify cell shape phenotypes associated with microenvironmental cues. *Biomaterials* 104:104–118
11. Jun I, Han HS, Edwards JR, Jeon H (2018) Electrospun fibrous scaffolds for tissue engineering: viewpoints on architecture and fabrication. *Int J Mol Sci* 19:E745
12. Khorshidi S, Mirzadeh A, Mazinani S, Lagaron JM, Sharifi S, Ramakrishna S (2016) A review of key challenges of electrospun scaffolds for tissue-engineering applications. *J Tissue Eng Regen Med* 10:715–738
13. Levensgood SL, Zhang M (2014) Chitosan-based scaffolds for bone tissue engineering. *J Mater Chem B* 2:3161–3184
14. Kim SB, Kim YJ, Yoon TL, Park SA, Cho IH, Kim EJ, Kim IA, Shin JW (2004) The characteristics of a hydroxyapatite-chitosan-PMMA bone cement. *Biomaterials* 25:5715–5723
15. Kim SE, Cho YW, Chung H, Jeong SY, Kwon ICL (2003) Porous chitosan scaffold containing microspheres loaded with transforming growth factor-beta1: implications for cartilage tissue engineering. *J Control Release* 91:365–374
16. Li Z, Ramay HR, Hauch KD, Xiao D, Zhang M (2005) Chitosan-alginate hybrid scaffolds for bone tissue engineering. *Biomaterials* 26:3919–3928

17. Xu HH, Jr CG (2005) Simon, Fast setting calcium phosphate-chitosan scaffold: mechanical properties and biocompatibility. *Biomaterials* 26:1337–1348
18. Yamane S, Iwasaki N, Majima T, Funakoshi T, Masuko T, Harada K, Minami A, Monde K, Nishimura S (2005) Feasibility of chitosan-based hyaluronic acid hybrid biomaterial for a novel scaffold in cartilage tissue engineering. *Biomaterials* 26:611–619
19. Sanchez-Alvarado DI, Guzman-Pantoja J, Paramo-Garcia U, Maciel-Cerda A, Martinez-Orozco RD, Vera-Graziano R (2018) Morphological study of Chitosan/Poly (vinyl alcohol) nanofibers prepared by electrospinning, collected on reticulated vitreous carbon. *Int J Mol Sci* 19:1718
20. Tamizi E, Azizi M, Dorraji MSS, Dusti Z, Azar VP (2017) Stabilized core/shell PVA/SA nanofibers as an efficient drug delivery system for dexpanthenol. *Polym Bull* 75:547–560
21. Jawalkar SS, Adoor SG, Sairam M, Nadagouda MN, Aminabhavi TM (2005) Molecular modeling on the binary blend compatibility of poly(vinyl alcohol) and poly(methyl methacrylate): an atomistic simulation and thermodynamic approach. *J Phys Chem B* 109:15611–15620
22. Ohkawa K, Cha D, Kim H, Nishida A, Yamamoto H (2004) Electrospinning of chitosan. *Macromol Rapid Commun* 25:1600–1605
23. Jia YT, Gong J, Gu XH, Kim HY, Dong J, Shen XY (2007) Fabrication and characterization of poly (vinyl alcohol)/chitosan blend nanofibers produced by electrospinning method. *Carbohydr Polym* 67:403–409
24. Tampieri A, Celotti G, Landi E, Sandri M, Roveri N, Falini G (2003) Biologically inspired synthesis of bone-like composite: self-assembled collagen fibers/hydroxyapatite nanocrystals. *J Biomed Mater Res A* 67:618–625
25. Kashiwazaki H, Kishiya Y, Matsuda A, Yamaguchi K, Iizuka T, Tanaka J, Inoue N (2009) Fabrication of porous chitosan/hydroxyapatite nanocomposites: their mechanical and biological properties. *Biomed Mater Eng* 19:133–140
26. Kong L, Gao Y, Lu G, Gong Y, Zhao N, Zhang X (2006) A study on the bioactivity of chitosan/nano-hydroxyapatite composite scaffolds for bone tissue engineering. *Eur Polym J* 42:3171–3179
27. Thein-Han WW, Misra RDK (2009) Three-dimensional chitosan-nanohydroxyapatite composite scaffolds for bone tissue engineering. *JOMJ Miner Metals Mater Soc* 61:41–44
28. Thein-Han WW, Misra RDK (2009) Biomimetic chitosan-nanohydroxyapatite composite scaffolds for bone tissue engineering. *Acta Biomater* 5:1182–1197
29. Shen K, Hu Q, Chen L, Shen J (2010) Preparation of chitosan bicomponent nanofibers filled with hydroxyapatite nanoparticles via electrospinning. *J Appl Polym Sci* 115:2683–2690
30. Celebi H, Gurbuz M, Koparal S, Dogan A (2013) Development of antibacterial electrospun chitosan/poly(vinyl alcohol) nanofibers containing silver ion-incorporated HAP nanoparticles. *Compos Interfaces* 20:1–14
31. Kundu B, Ghosh D, Sinha MK, Sen PS, Balla VK, Das N, Basu D (2013) Doxorubicin-intercalated nanohydroxyapatite drug-delivery system for liver cancer: an animal model. *Ceram Int* 39:9557–9566
32. Kataria K, Gupta A, Rath G, Mathur RB, Dhakate SR (2014) In vivo wound healing performance of drug loaded electrospun composite nanofibers transdermal patch. *Int J Pharm* 469:102–110
33. Baghersad S, Hajir Bahrami S, Mohammadi MR, Mojta-hedi MRM, Milan PB (2018) Development of biodegradable electrospun gelatin/aloe-vera/poly( $\epsilon$ -caprolactone) hybrid nanofibrous scaffold for application as skin substitutes. *Mater Sci Eng C Mater Biol Appl* 93:367–379
34. Bodhak S, Bose S, Bandyopadhyay A (2009) Role of surface charge and wettability on early stage mineralization and bone cell-materials interactions of polarized hydroxyapatite. *Acta Biomater* 5:2178–2188
35. Ghosh A, Raha S, Dey S, Chatterjee K, Chowdhury AR, Barui A (2019) Chemometric analysis of integrated FTIR and Raman spectra obtained by non-invasive exfoliative cytology for the screening of oral cancer. *Analyst* 144:1309–1325
36. Wei W, Wang X, Wang Y, Xu M, Cui J, Wei Z (2013) Evaluation of removal efficiency of fluoride from aqueous solution using nanosized fluorapatite. *Desalin Water Treat* 52:6219–6229
37. Silva SML, Braga CRC, Fook MVL, Raposo CMO, Carvalho LH, Canedo EL (2012) Application of infrared spectroscopy to analysis of chitosan/clay nanocomposites. In: Theophile T (ed) *Infrared spectroscopy – materials science, engineering and technology*. InTech, pp 43–62
38. Alhosseini SN, Moztaaradeh F, Mozafari M, Asgari S, Dodel M, Samadikuchaksaraei A, Kargozar S, Jalali N (2012) Synthesis and characterization of electrospun polyvinyl alcohol nanofibrous scaffolds modified by blending with chitosan for neural tissue engineering. *Int J Nanomed* 7:25–34
39. Alobeedallaha H, Ellis JL, Rohanizadeh R, Costera H, Dehghania F (2011) Preparation of nanostructured hydroxyapatite in organic solvents for clinical applications. *Trends Biomater Artif Organs* 25:12–19
40. Teng SH, Lee EJ, Yoon BH, Shin DS, He HE, Oh JS (2009) Chitosan/nanohydroxyapatite composite membranes via dynamic filtration for guided bone regeneration. *J Biomed Mater Res A* 88:569–580
41. Abdeen Z, Mahmoud MS, Mohammad SG (2015) Adsorption of Mn(II) ion on polyvinyl alcohol/chitosan dry blending from aqueous solution. *Environ Nanotechnol Mon Manage* 3:1–9
42. Wang L, Li C (2007) Preparation and physicochemical properties of a novel hydroxyapatite/chitosan-silk fibroin composite. *Carbohydr Polym* 68:740–745

43. Tan J, Yie Z, Zhang XW (2011) Influence of chitosan on electrospun PVA nanofiber. *Mat Adv Mater Res* 311–313:1763–1768
44. Fu C, Bai H, Zhu J, Niu Z, Wang Y, Li J, Yang X, Bai Y (2017) Enhanced cell proliferation and osteogenic differentiation in electrospun PLGA/hydroxyapatite nanofibre scaffolds incorporated with graphene oxide. *PLoS One* 12:e0188352
45. Ganesh M, Aziz AS, Ubaidulla U, Hemalatha P, Saravanakumar A, Ravikumar R, Peng MM, Choi EY, Jang HT (2016) Sulfanilamide and silver nanoparticles-loaded polyvinyl alcohol-chitosan composite electrospun nanofibers: synthesis and evaluation on synergism in wound healing. *Ind Eng Chem* 39:127–135
46. Santos C, Clarke RL, Braden M, Guitian F, Davy KWM (1897) Water absorption characteristics of dental composites incorporating hydroxyapatite filler. *Biomaterials* 2002:23
47. Correlo VM, Pinho ED, Pashkuleva I, Bhattacharya M, Neves NM, Reis RL (2007) Water absorption and degradation characteristics of chitosan-based polyesters and hydroxyapatite composites. *Macromol Biosci* 7:354–363
48. Reis RL, Mendes SC, Cunha AM, Bevis MJ (1997) Processing and In-vitro degradation of starch/EVOH thermoplastic blends. *Polym Int* 43:347
49. Vaz CM, Cunha AM, Reis RL (2001) Chemical modification of starch based biodegradable polymeric blends: effects on water uptake, degradation behaviour and mechanical properties. *Mater Res Innov* 4:375
50. Demirgoz D, Elvira C, Mano JF, Cunha AM, Piskin E, Reis RL (2000) In vitro degradation behaviour of starch/EVOH biomaterials. *Polym Degrad Stab* 70:161
51. Araujo MA, Vaz CM, Cunha AM, Mota M (2001) Degradation model of starch-EVOH + HA composites. *Polym Degrad Stab* 73:237
52. Shih H, Lin CC (2012) Crosslinking and degradation of step-growth hydrogels formed by thiol-ene photo-click chemistry. *Biomacromol* 13:2003–2012
53. Wenz A, Borchers K, Tovar GEM, Kluger PJ (2017) Bone matrix production in hydroxyapatite-modified hydrogels suitable for bone bioprinting. *Biofabrication*. 9:044103



**Ms. Aishwarya Satpathy** completed her Masters of Technology (M.Tech.) dissertation project in the field of Biomedical Engineering jointly at Indian Institute of Engineering Science and Technology (IEST), Shibpur, Kolkata, India and CSIR-Central Glass and Ceramic Research Institute (CSIR-CGCRI), Kolkata, India She completed her Bachelor of Technology (B.Tech.) in biotechnology from National Institute of Technology (NIT), Durgapur, India. Ms. Satpathy has published two research articles in peer reviewed international journals.



**Dr. Aniruddha Pal** is an experienced polymer chemist currently working as a National Postdoctoral Fellow at CSIR—Central Glass and Ceramic Research Institute, Kolkata, India. Dr. Pal obtained his undergraduate degree from Ramakrishna Mission Vivekananda Centenary College, Rahara, India and postgraduate degree from Indian Institute of Technology (Indian School of Mines) Dhanbad, India in 2011 and 2013, respectively. He earned his PhD degree in Polymer Chemistry at Indian Institute of Technology (Indian School of Mines) Dhanbad, India in 2018. His Ph.D. dissertation work was focused on the synthesis of functional polymer/hydrogels via control radical polymerization technique for potential application in waste water treatment and drugs delivery system. His current post-doctoral research work is focused on development of injectable hydrogels for sustained delivery of therapeutic protein and stem cells for potential applications in bone tissue engineering and regenerative medicines. Dr. Pal has published 11 research articles in reputed international journals like Carbohydrate Polymers, Journal of Colloid and Interface Science, Polymer etc. His research interest is primarily focused in development of polymeric biomaterials for drug delivery and tissue engineering applications.



**Dr. Somoshree Sengupta** obtained her PhD in life science from the Academy of Scientific and Innovative Research (AcSIR), CSIR-Central Glass and Ceramic Research Institute, Kolkata in 2019. She received her undergraduate degree (B.Sc) in Microbiology from the Pune University, Pune, India and Masters degree (M.Sc) in Microbiology from Amity University, Delhi, India in the year 2009. She has published 14 SCI journal papers and received CSIR-SRF in 2013 and DST woman scientist fellowship in the year 2017. Her area of expertise includes molecular biology, drug delivery and nanotechnology.

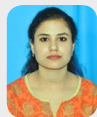


**Ms. Ankita Das** is pursuing her Ph.D in Stem cells and Regenerative Medicine at Indian Institute of Engineering Science and Technology, Shibpur. She completed her Masters (M.Sc.) dissertation project in the field of structural biology at Ballygunge Science College, University of Calcutta. She had completed her Bachelor of Science (B.Sc) in Microbiology from Scottish Church College, Kolkata where she participated in the 6th one day workshop on Biotechnology at University of Calcutta, supported by NASI. Ms. Ankita authored a journal paper titled “Aberration in the structural paradigm of lens protein  $\alpha$  crystalline by UV-C irradiation”, in Applied Biological Chemistry.



**Md. Mahfujul Hasan** is a Scientific Officer in the Institute of Glass & Ceramic Research and Testing (IGCRT), at the Bangladesh council of scientific and industrial research (BCSIR), Dhaka, Bangladesh. Mr. Hasan received his Undergraduate and Masters degree in ‘Applied Chemistry & Chemical Engineering’ from Rajshahi University, Bangladesh in 2010 and 2011,

respectively. His research interest is primarily focused on the development of ecofriendly high performance and self-cleaning nano ceramics coatings on glass substrate for structural engineering applications. He is a life member of the Bangladesh Ceramic Society, Bangladesh Chemistry Society, Network and Instrument Technical Personnel and User Scientist of Bangladesh (NITUB).



**Ms. Itishree Ratha** is pursuing her Ph.D in Science at the Academy of Scientific and Innovative Research (AcSIR) in the CSIR-Central Glass and Ceramic Research Institute, Kolkata. She has been awarded CSIR-SRF fellowship in 2019 in support of her

PhD research work. She received her undergraduate degree (B.Sc) in Chemistry from Sambalpur University, Odisha, India in 2010 and Masters degree (M.Sc) in Chemistry from NIT Rourkela, Odisha, India in 2012. She has published 4 SCI journal articles and received CSIR-SRF in 2019. Her area of expertise includes bioceramics, drug delivery and nanotechnology.



**Dr. Ananya Barui** is an Assistant Professor of biomedical Engineering in the Centre for Healthcare Science and Technology at Indian Institute of Engineering Science and Technology, Shibpur since 2012. She received her PhD degree in 2011 from Indian institute of

Technology, Kharagpur. Her research interest is development of integrated analytical systems based on functional microscopy and spectroscopy for early diagnosis of cancers.



**Dr. Subhadip Bodhak** is working as a Senior Scientist in the Bioceramics & Coating Division of CSIR-Central Glass and Ceramic Research Institute, Kolkata, India since 2017. His past and present research endeavors are primarily in the field of Biomaterials Science

and Tissue Engineering. His research interest is focused on developing functional biomaterials for musculoskeletal tissue regeneration by utilizing effective strategies that combine knowledge from material science, chemistry & biology. Dr. Bodhak was born in Kolkata, India, in 1982. He received his B.Tech. in Ceramic Eng. from University of Calcutta, India in

2004, M.Tech. in Materials Eng. from IIT Kanpur, India in 2006 and PhD in Materials Science from Washington State University, USA in 2010. After finishing PhD, Dr. Bodhak was accepted for prestigious 'JSPS Fellowship' at the National Institute for Materials Science (NIMS) in Japan in 2010 and National Research Council (NRC) Fellowship jointly at the National Institute of Standards & Technology (NIST) and National Institute of Health (NIH), Maryland, USA in 2012. In 2015 after his postdoctoral tenure, Dr. Bodhak joined in the innovation center of Evonik Corporation, AL, USA as a materials scientist and contributed in the cutting edge medical device development that has been successfully commercialized as a product. Among many scholastic awards, Dr. Bodhak has been awarded "Ramalingaswami Re-Entry Fellowship Award" funded by Department of Biotechnology (DBT), Government of India in 2017; "Starting Investigator Research Grant" funded by Science Foundation Ireland (SFI) in 2014; "Outstanding Presenter Award" at the Asian BioCeramics Symposium, Tsukuba, Japan in 2011; "Acta Student Award" and \$2000 scholarship" in recognition of best student-authored paper published in Acta Biomaterialia in 2009; "Academic Excellence Award" given by Indian Institute of Technology Kanpur, India in 2005; "Best Project Award-2004" given by Indian Refractory Makers Association in 2004 and "Prof Sasadhar Ray Memorial Committee Certificate of Proficiency in Ceramic Technology" in recognition of 1st place ranking in undergraduate class during 2000-2004. Dr. Bodhak is author of 35 scholarly articles including leading journals like Biomaterials; 3 international patent applications; cited over 900 times and delivered more than 19 invited/contributory lectures in several national and international conferences across the world. Dr. Bodhak is currently serving as an expert reviewer for research proposals submitted under Marie Skłodowska-Curie COFUND Fellowship scheme in Medical Device Research at CÚRAM, Centre for Research in Medical Devices, Ireland along with several leading journals in biomaterials field and an Editorial-board member in the "Frontiers in Mechanical Engineering: Computer-Aided and Digital Manufacturing Technologies" journal, Frontiers Publication Inc., EPFL, Lausanne, Switzerland. He is an elected member of Sigma XI: The Scientific Research Society, USA and life member of Indian JSPS Alumni Association.